PHYSICAL REVIEW C VOLUME 30, NUMBER 5 NOVEMBER 1984

Tritium form factors at low q

D. H. Beck, S. B. Kowalski, M. E. Schulze,* and W. E. Turchinetz
Department of Physics and Laboratory for Nuclear Science, Massachusetts Institute of Technology, Cambridge, Massachusetts 02139

J. W. Lightbody, Jr., X. K. Maruyama, and W. J. Stapor†
National Bureau of Standards, Washington, D.C. 20234

H. S. Caplan, G. A. Retzlaff, and D. M. Skopik
Department of Physics and Saskatchewan Accelerator Laboratory, University of Saskatchewan, Saskatoon, Saskatchewan, Canada S7N 0W0

R. Goloskie
Department of Physics, Worcester Polytechnic Institute, Worcester, Massachusetts 01601
(Received 9 July 1984)

The elastic charge and magnetic form factors of ^{3}H have been measured in the region $0.0477 < q^2 < 2.96$ fm^{-2}. Throughout this range, the charge form factor is found to be larger than previous measurements, whereas the magnetic form factor agrees with the earlier work. The change in the charge form factor slightly increases the discrepancy between the calculated and observed binding energy difference between ^{3}H and ^{3}He.

I. INTRODUCTION

Elastic scattering of electrons was used in this experiment to measure the charge and magnetic form factors of ^{3}H. At low momentum transfers these observables are approximately the Fourier transforms of the one-body charge and current densities of the nucleus. We have measured the charge form factor ($C0$) at eight points and the magnetic form factor ($M1$) at four points in the range of momentum transfer $0.0477 \leq q^2 \leq 2.96$ fm^{-2}. Previous experiments[1,2] determined these form factors in the range $0.29 \leq q^2 \leq 8.0$ fm^{-2} (charge) and $1.0 \leq q^2 \leq 8.0$ fm^{-2} (magnetic).

The structure of the bound state of three nucleons is a fundamental question in nuclear physics. The particular motivation for studying the trinucleon ground state at this time is that, in principle, one can now calculate the binding energy and wave functions exactly (for a given NN interaction) using the Faddeev theory. In practice, there are deficiencies in the results because the Faddeev equations are nonrelativistic, and because our understanding of both the NN potentials and to a lesser extent the nucleon form factors is incomplete. Variational calculations, now in good agreement with similar Faddeev calculations, have also been illuminating. For example, three-nucleon effects can be included in the Hamiltonian because they are relatively less complicated.

At higher momentum transfers ($q^2 \geq 12$ fm^{-2}) meson exchange currents (MEC's) dominate the form factors. For the region of low momentum transfer explored in this experiment, the MEC's are unimportant in the charge form factor and contribute only about 15% to the magnetic form factor. Furthermore, because the MEC's contributing to F_m are isovector and of the same relativistic order as the one-body operator, they are confidently predicted.[3–5] In this q region, then, there certainly is a substantial, if not fully determined, microscopic calculation of the quantities measured in this experiment. We compare our results to these theories in Sec. IV.

We can also examine the details of our understanding of simple nuclear systems in a somewhat different way. The binding energy difference $\Delta M_B = B_{^3\mathrm{H}} - B_{^3\mathrm{He}}$ is known very accurately (± 0.21 keV) to be 764 keV. As expected, the largest contribution is the difference in Coulomb energy—about 640 keV. There are other contributions to be taken into account, including the dynamical effect of the n-p mass difference, differences in magnetic interactions (spin and current), relativistic corrections, and exchange currents. However, these contributions leave the calculated binding energy difference 40—80 keV short of the measured value.[6,7] This discrepancy has been interpreted as evidence for charge symmetry breaking in the NN potential.

The Coulomb energy contribution may be determined from the measured charge form factors of ^{3}H and ^{3}He (Refs. 8 and 9) as

$$\Delta E_C = \frac{2\alpha}{\pi\sqrt{3}} \int_0^\infty dq\, G_p{}^2(\tfrac{1}{3}q^2) \times [\tfrac{4}{3}F_{\mathrm{He}}(q^2) - \tfrac{1}{3}F_{\mathrm{H}}(q^2)]/G_{\mathrm{p}}(q^2)\,,$$

where G_{p} is the proton charge form factor and F_{H} and F_{He} are the ^{3}H and ^{3}He charge form factors, respectively. This formula uses the spatial symmetry of the wave functions demanded by the Pauli principle and assumes that

the neutron charge form factor is zero. Since the contribution to the integral from the region $0 = \leq q^2 \leq 6$ fm^{-2} is larger than 90%,[10] the data from this experiment may be directly used to calculate the Coulomb energy difference (Sec. IV).

II. APPARATUS

A. MIT Bates

The measurements in the range $0.256 \leq q^2 \leq 2.96$ fm^{-2} were made at the MIT-Bates Linear Accelerator Center using the single pass beam (maximum energy nominally 400 MeV). The beam energy was measured to an accuracy of about $\pm 0.5\%$ in this experiment. Scattered electrons were detected using the dispersion matched energy loss spectrometer system (ELSSY) which is fully described in Refs. 11–13.

The beam charge was measured by a pair of toroids which have been calibrated to an absolute accuracy of 0.1% and were periodically recalibrated. In front of the spectrometer and about 2 m from the target chamber, a pair of slits define the solid angle acceptance. The height and width of the opening were measured to ± 0.076 mm corresponding to an error of about $\pm 0.8\%$ at the smallest solid angle opening used in this experiment (0.042 msr). Peak beam currents and solid angles were limited to keep the measured detector dead time below 10%.

B. NBS

The two lowest q points were taken at the National Bureau of Standards (NBS) electron linear accelerator. The beam current was measured with a toroid calibrated with a Faraday cup. Scattered electrons were momentum analyzed in a 169.8° double focusing magnetic spectrometer and detected in a 48 detector hodoscope of Si(Li) solid state detectors in coincidence with two plastic scintillators. The details of this system are given in Ref. 14.

C. Target

The target was ^{3}H dissolved in a thin titanium and copper metal foil, made at the Isotope Division of Oak Ridge National Laboratory. The copper was evaporated to a thickness of 1.97 mg/cm^2 on a 2.18 mg/cm^2 titanium foil in order to improve the thermal conductivity. The foil was then warmed to about 450 °C and exposed to $^3H_2$ gas. The result is a material which is partly a solution of gaseous hydrogen in the solid metal and partly the compound TiH_2.

Unfortunately, the foil was wrinkled and consequently its absolute ^{3}H areal density was not known. Relative normalization from setup to setup was done by measuring elastic scattering from Ti and Cu with the ^{3}H target and with a flat "blank" target cut from the same piece of Ti-Cu stock. The effective thickness of the ^{3}H target varied from 1.10–1.35 times the thickness of the blank due to changes in the size of the beam spot (principally changes in the width; the dimension perpendicular to the dispersion direction).

Absolute normalization of the target thickness was accomplished by measuring elastic proton scattering at 13.6 MeV and 140°. This experiment was done using the Triangle Universities Nuclear Laboratory (TUNL) Tandem Van de Graaff at Duke University. Scattered protons were detected (stopped) with two silicon surface barrier detectors on either side of the target in the horizontal plane. They were mounted inside the scattering chamber, 15 cm away from the target with apertures in front of them limiting the solid angle acceptance to 0.411 msr. The ^{3}H cross section was again normalized to the blank as was done in the electron experiment. Comparison with the results of Detch *et al.*[15] (0.5% experimental error) gave a ^{3}H thickness of 0.217 ± 0.009 mg/cm^2 for this target.

Average currents at MIT-Bates were limited to be < 25 μA due to experience at Saskatoon with a similar ^{1}H tar-

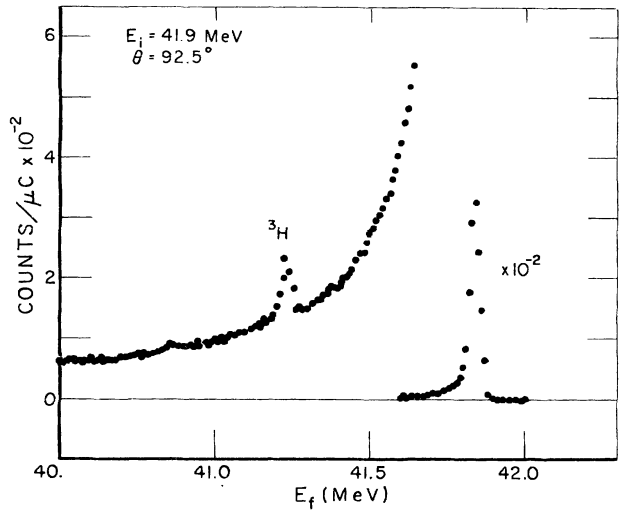

FIG. 1. Spectrum of scattered electrons measured at NBS.

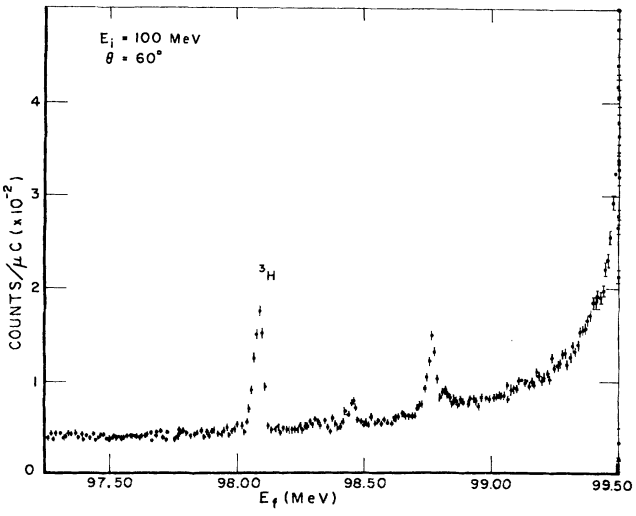

FIG. 2. Spectrum of scattered electrons measured at Bates. Structure was not observed near the ^{3}H elastic peak when the blank TiCu foil was measured for any of the NBS or Bates spectra.

TABLE I. ^{3}H elastic scattering cross sections.

E_i (MeV)	θ (deg)	q^2 (fm^{-2})	$\frac{d\sigma}{d\Omega}$ (cm^2/sr)	Place
29.85	93.1	0.0477	$9.30 \pm 0.55 \times 10^{-30}$	NBS
41.85	93.1	0.0934	$5.53 \pm 0.30 \times 10^{-30}$	NBS
29.85	162.5	0.0876	$2.79 \pm 0.21 \times 10^{-31}$	NBS
100.0	60.0	0.252	$5.72 \pm 0.21 \times 10^{-30}$	MIT
150.0	60.0	0.563	$2.000 \pm 0.029 \times 10^{-30}$	MIT
77.0	160.0	0.561	$8.04 \pm 0.93 \times 10^{-32}$	MIT
205.0	60.0	1.04	$7.91 \pm 0.24 \times 10^{-31}$	MIT
247.0	60.0	1.50	$3.46 \pm 0.19 \times 10^{-31}$	MIT
127.0	160.0	1.48	$2.37 \pm 0.20 \times 10^{-32}$	MIT
300.0	60.0	2.20	$1.306 \pm 0.043 \times 10^{-31}$	MIT
350.0	60.0	2.96	$5.34 \pm 0.18 \times 10^{-32}$	MIT
183.0	160.0	2.96	$5.55 \pm 0.43 \times 10^{-33}$	MIT

get.[16] Currents up to 15 μA concentrated in a spot about ten times smaller than that at MIT-Bates resulted in no detectable loss of hydrogen from the target. Beam currents at NBS were <2 μA and <75 nA at TUNL.

Since these targets were 3.8 cm in diameter, the vertical beam spot size on the target of about 4.0 cm required for full dispersion correction at MIT-Bates could not be used. Using spots that were typically 2.5 cm high reduced the best resolution to about 8×10^{-4}. The resolution at NBS was 10^{-3}.

III. ANALYSIS

Typical spectra for the tritiated target are shown in Figs. 1 and 2. For background subtractions the blank target spectra were normalized to the corresponding ^{3}H target spectra using the Ti and Cu elastic peak areas and requiring that the radiatively corrected cross sections be independent of the cutoff energy. At the higher incident energies the large kinematic recoil of ^{3}H resulted in the Ti and Cu peaks being shifted off the edge of the focal plane detectors. In these cases the normalization was done by using the Ti and Cu radiation tails of each target, at much lower inelasticity than the ^{3}H elastic peak region.

The data taken at MIT-Bates were analyzed in two ways. First, the area ($d\sigma/d\Omega$) of the ^{3}H elastic peak was determined by summing the counts in the appropriate energy region after a background subtraction was made. Second, the elastic peaks were fit with a composite peak function and a polynomial background.[17] These two methods agreed to within the statistical error in all cases except for the highest and lowest energy runs. In these instances the average of the two values was used, with the error being increased conservatively to include both values. The two lowest q points (NBS) were analyzed only by fitting since the ^{3}H target, but not the blank target, became slightly oxidized between the times of the MIT-Bates and NBS runs.

In all cases the cross sections were corrected for radiative effects using the formula of Mo and Tsai.[18] The results are given in Table I. The errors only include statistical errors from the number of counts in the ^{3}H peak and the relative normalization error.

According to the Rosenbluth cross section for electron

TABLE II. ^{3}H charge and magnetic form factors which include contributions of random (r) and systematic (s) measurement errors.

q^2_{eff} (fm^{-2})	F_c	$\Delta F_{c,r}$	$\Delta F_{c,s}$	$\Delta F_{c,t}$	F_m	$\Delta F_{m,r}$	$\Delta F_{m,s}$	$\Delta F_{m,t}$
0.0510	0.967	0.029	0.036					
0.0980	1.039	0.038	0.029	0.048	1.086	0.100	0.061	0.117
0.258	0.950	0.017	0.022	0.028				
0.571	0.826	0.019	0.013	0.023	0.806	0.062	0.023	0.066
1.05	0.697	0.011	0.016	0.019				
1.51	0.548	0.011	0.009	0.014	0.473	0.023	0.012	0.026
2.21	0.387	0.006	0.009	0.011				
2.98	0.282	0.007	0.006	0.009	0.260	0.011	0.007	0.013
	Resorted Saskatoon data (Ref. 2)							
0.30	0.872			0.041				
0.50	0.782			0.036				
0.70	0.785			0.030				
0.90	0.659			0.023				

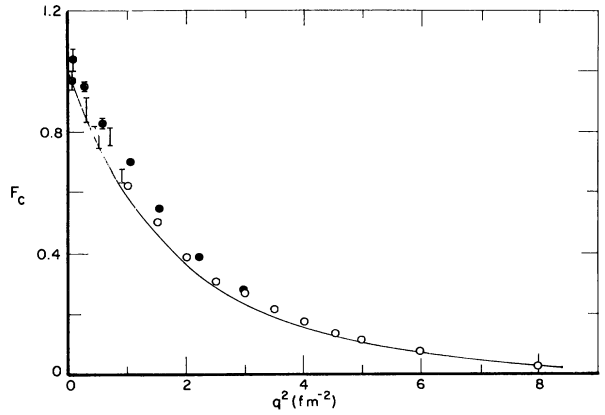

FIG. 3. ^{3}H charge form factors: (●)—present experiment; (○)—Ref. 1; I—Ref. 2. The solid line is the calculation of Ref. 25.

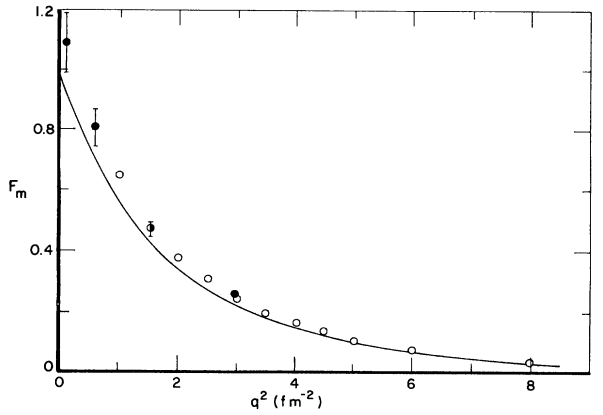

FIG. 4. ^{3}H magnetic form factors: (●)—present experiment; (○)—Ref. 1. The solid line is the calculation of Ref. 3.

scattering from extended spin $\frac{1}{2}$ objects,

$$\frac{d\sigma}{d\Omega}=\sigma_{\text{Mott}}\frac{1}{\eta}\left[\frac{F_c^2}{1+\tau}+\tau\mu_A^2F_m^2\left[\frac{1}{1+\tau}+2\tan^2\frac{\theta}{2}\right]\right],$$

where

$$\sigma_{\text{Mott}}=\frac{Z^2e^4}{4E_i^2}\frac{\cos^2\theta/2}{\sin^4\theta/2},$$

$$\eta=1+\frac{2E_i}{M}\sin^2\theta/2, \text{ the recoil factor},$$

$$\tau=\frac{q^2}{4M^2},$$

$$\mu_A=8.94=\frac{A}{Z}\mu(^3\text{H}),$$

and the form factor normalization is defined as

$$F_c(q=0)=F_m(q=0)=1.0.$$

The results are presented in Table II. For the cases where a corresponding back angle measurement was not made, a fit to the magnetic form factors of Ref. 1 was used in extracting the charge form factors from the forward angle cross sections. For the cases of corresponding q where the momentum transfers were not precisely the same, the measured cross sections were adjusted using a Taylor series expansion in energy.

Because the electron waves are distorted near the nucleus, the momentum transfer is increased. This change may be taken into account with an effective momentum transfer

$$q_{\text{eff}}=q\left[1+\frac{3}{2}\frac{Ze^2}{E_ir_{\text{eq}}}\right],$$

where $r_{\text{eq}}=\sqrt{(5/3)}\langle r^2\rangle^{1/2}$ is the radius of the equivalent hard sphere. At the lowest energy used in this experiment, 30 MeV, the effective momentum transfer is only 3% larger than q; therefore, at most, this is a small correction.

The uncertainties associated with the form factors that we have determined are due to both random and systematic errors in the experiment. The systematic errors for the spectrometer systems are discussed in detail in Refs. 11 and 14; they are at the one percent level. The systematic error which completely dominates this experiment is the 4.1% error in the cross section due to the uncertainty in the target thickness. The total form factor errors (random plus systematic added in quadrature) are shown in Table II.

Finally, we note that in all cases except for the 183 MeV, 160° run, carbon cross sections were measured in order to determine the overall accuracy of the experiment. The carbon cross sections agree with a standard phase shift calculation and the results of Ref. 19.

IV. RESULTS AND DISCUSSION

The charge and magnetic form factors are shown with the data of Refs. 1 and 2 in Figs. 3 and 4. The form fac-

TABLE III. Comparison of the Fourier-Bessel analysis of the charge form factors for ^{3}He and ^{3}H.

	$q_{\max}$ (fm^{-1})	N	R (fm)	χ^2	$\frac{4\pi}{Z}\int_0^\infty r^2\rho(r)dr$	$\langle r^2\rangle^{1/2}$ fm
^{3}He	7[a]	12	5.0	2.75	0.995	1.88±0.02
	2.8	4	4.4	3.09	0.993	1.87±0.03
^{3}H	2.8	3	3.5	3.41	1.018	1.68±0.03

[a]Reference 21.

tors of Ref. 2 have been resorted into larger q^2 intervals in order to reduce the density of points and the relative error bars; these resorted data are given in Table II. Whereas the magnetic form factors agree with the earlier work, we find that the charge form factors reported here are systematically larger, the deviation decreasing with increasing q. At $q^2=1.0$ fm^{-2}, the form factor of Ref. 1, for example, is more than three standard deviations below that of this experiment (with systematic error added in quadrature to the random error).

Two fitting procedures were employed to derive an rms charge radius from the data. Because

$$F(q)=4\pi\int_0^\infty \rho(r)j_0(qr)r^2dr\ ,$$

the data may be fitted to a power series in q^2 as,

$$F(q)=1-\frac{1}{3!}q^2\langle r^2\rangle+\frac{1}{5!}q^4\langle r^4\rangle-\cdots=\sum_{\nu=1}^{N}a_\nu q^{2(\nu-1)}\ , \tag{1}$$

with the rms radius being given by $\langle r^2\rangle^{1/2}=\sqrt{-6a_1}$. The errors were determined in this case by finding the intersection of the $\chi^2_{\text{best}}+1$ and χ^2 surface in the fitting parameter space, due to lack of orthogonality in the basis functions.

The Fourier-Bessel (FB) fitting procedure of Dreher *et al.*[20] was also used. Here,

$$\rho(r)=\sum_{\nu=1}^{8}a_\nu j_0(q_\nu r),\quad r<R \tag{2}$$

and

$$\rho(r)\equiv 0\ ,\quad r\geq R$$

where $j_0(q_\nu r)$ is the 0th order spherical Bessel function and $j_0(q_\nu R)=0$ occurs for $q_\nu R=\nu\pi$. It follows that

$$F(q)=-\sum_{\nu=1}^{N}4a_\nu G_\nu(q)\ , \tag{3}$$

where the quantities

$$G_\nu=\frac{\sin(qR)}{\nu q j_1(\nu\pi)(q^2-q_\nu^2)}$$

form the basis functions for the fitting procedure. The N simultaneous equations for a_ν were found by minimizing the χ^2 and then solved using matrix methods. The advantage of this fitting procedure is that the errors of the fit are unambiguously determined since the G_ν's are orthogonal functions. Hence, by using Eq. (2) and calculating

$$\langle r^2\rangle=4\pi\int_0^\infty r^4\rho(r)dr\ ,$$

the rms radius was determined. The standard deviation of $\langle r^2\rangle$ is found from

$$\sigma_{\langle r^2\rangle}=\sum_{i,j}\epsilon_{ij}\frac{\partial\langle r^2\rangle}{\partial a_i}\frac{\partial\langle r^2\rangle}{\partial a_j}\ ,$$

where ϵ_{ij} is the full error matrix of the least squares fit.

Since the largest q for which the ^{3}H form factor has been measured is only 2.82 fm^{-1}, we have investigated how sensitive the radius determination is to the limited q

TABLE IV. Expansion coefficients [Eqs. (1) and (3)].

Type of fit	Charge[a]	Charge[b]	Charge[c]	Charge[d]	Magnetic[a]	Magnetic[b]
a_1	(1.026±0.017)	(2.565±0.018)×10^{-2}	(1.032±0.006)	(4.967±0.047)×10^{-2}	(1.051±0.022)	(2.660±0.054)×10^{-2}
a_2	(−4.794±0.036)×10^{-1}	(3.485±0.028)×10^{-2}	(−3.977±0.009)×10^{-1}	(2.66 ±0.67)×10^{-2}	(−5.258±0.042)×10^{-1}	(3.323±0.035)×10^{-2}
a_3	(1.051±0.005)×10^{-1}	(1.554±0.069)×10^{-2}	(5.728±0.014)×10^{-2}	(2.544±0.322)×10^{-2}	(1.216±0.004)×10^{-1}	(1.685±0.056)×10^{-4}
a_4	(−1.168±0.003)×10^{-2}		(−2.906±0.027)×10^{-3}		(−1.381±0.001)×10^{-4}	
a_5	(5.104±0.006)×10^{-4}				(6.061±0.089)×10^{-4}	
χ^2	3.64	3.41	1.04	1.02	0.767	0.788
r (fm)	1.67±0.02	1.68±0.03	1.52±0.01	1.56±0.05	1.73±0.02	1.72±0.06
R (fm)		3.50		2.60		3.41

[a]Power series—all data.
[b]Fourier-Bessel—all data.
[c]Power series—this experiment and data of Ref. 1 for $q^2\geq 3.5$ fm^{-2}.
[d]Fourier-Bessel—this experiment and data of Ref. 1 for $q^2\geq 3.5$ fm^{-2}.

range by comparing it to ^{3}He. The charge radius of ^{3}He has been determined by this method to be 1.877 ± 0.019 fm when a wide range of data were used ($q_{max}\sim7$ fm^{-1}).[21] We have reanalyzed the ^{3}He form factors with a data set that was limited to values of $q\leq2.82$ fm, the same range of data available for ^{3}H. Table III summarizes the comparison of ^{3}H and ^{3}He for the Fourier-Bessel analysis. The conclusion is that the radius is reasonably well determined by form factor measurements for $q\leq3$ fm^{-1}.

Using both methods we have also fitted just the new charge form factor data to determine by how much these data indicate that the rms radius of ^{3}H could be changed. In order that the polynomial fit not be restricted to a few terms and because the Fourier-Bessel fitting procedure is not appropriate for only low q data, we have included the points of Ref. 1 for $q^2>3.5$ fm^{-2}. Table IV summarizes all of our fitting results.

In comparing the charge and magnetic form factors to the exact calculations discussed in the Introduction, the tendency of these models to overestimate the size of the three-body nuclei is evident (Figs. 3 and 4). If this is directly connected to the underbinding of these nuclei, as seems likely, it is probably more instructive to look at the difference in the rms charge radii. Calculations[22] are able to reproduce reasonably well the ratio between the two radii of about 1.70:1.90 [$r_C(^3\text{H}):r_C(^3\text{He})$] using the ^{3}H radius of Ref. 1. Since the difference between $r_C(^3\text{H})$ and $r_C(^3\text{He})$ is due primarily to the size of the S' state admixture[22] ($L=0$, mixed spatial symmetry), the current results could suggest either a different S' strength[23] or another space asymmetric contribution to the wave function.

The results of this experiment were used to recalculate the Coulomb contribution to the binding energy difference between ^{3}He and ^{3}H ($\Delta M_B\sim764$ keV). The data of Refs. 1 and 2 yield $\Delta E\sim640$ keV, whereas the new data lower this value by ≈25 keV.[24]

Two recent experiments indicate then that the Coulomb contribution remains unchanged or is slightly lowered, thus the hope that the shortfall in $\Delta M_B(40-80)$ was due to an error in the ^{3}H charge form factor is not borne out. There remains, therefore, the question of a charge asymmetry in the NN force large enough to explain this difference.

V. SUMMARY

In this experiment the elastic charge and magnetic form factors of ^{3}H were measured in the range $0.0477\leq q^2\leq2.96$ fm^{-2} using electron scattering. Whereas the magnetic form factor measured in the current experiment agrees with earlier work, the charge form factor does not. It is systematically larger than the older measurement, particularly at the lowest common momentum transfer. This indicates a smaller charge "size" for ^{3}H than previously thought. These results also marginally increase the discrepancy between the measured binding energy difference between ^{3}H and ^{3}He of 764 keV and the calculated value since the Coulomb energy difference, the largest contribution to the binding energy difference, decreases when these data are used in the calculation.

The Fourier-Bessel and power series fitting procedures gave essentially the same charge and magnetic radii. Since the errors associated with the Fourier-Bessel method are the least model dependent, we quote the radii and errors for it; namely, the charge radius of ^{3}H using all the available data is 1.68 ± 0.03 fm, and the magnetic radius is 1.72 ± 0.06 fm.

ACKNOWLEDGMENTS

We wish to thank S. King, D. Wagenaar, and H. Weller of Duke University for their assistance in the ^{3}H(p,p) measurement and J. L. Friar and E. L. Tomusiak for many helpful discussions. This work was supported in part by the U. S. Department of Energy, Contract EY-76-C-02-3069, and by the Natural Sciences and Engineering Research Council of Canada.

*Permanent address: Department of Physics, Syracuse University, Syracuse, NY 13210.

†Was also at The Catholic University of America, Washington, D.C.; now at Naval Research Laboratory, Washington, D.C.

[1]H. Collard *et al.*, Phys. Rev. **138**, B57 (1965).

[2]D. H. Beck, J. Asai, and D. M. Skopik, Phys. Rev. C **25**, 1152 (1982).

[3]E. Hadjimichael, B. Goulard, and R. Bornais, Phys. Rev. C **27**, 831 (1983), and (private communication).

[4]J. L. Friar, Ann. Phys. (N.Y.) **104**, 380 (1977).

[5]M. Chemtob and M. Rho, Nucl. Phys. **A163**, 1 (1971).

[6]R. A. Brandenburg, S. A. Coon, and P. U. Sauer, Nucl. Phys. **A294**, 305 (1978).

[7]J. L. Friar (private communication).

[8]J. L. Friar, Nucl. Phys. **A156**, 43 (1970).

[9]M. Fabre de la Ripelle, Prog. Theor. Phys. **40**, 1454 (1968).

[10]J. L. Friar and B. F. Gibson, Phys. Rev. C **18**, 908 (1978).

[11]P. C. Dunn *et al.*, Phys. Rev. C **27**, 71 (1983).

[12]W. Bertozzi *et al.*, Nucl. Instrum. Methods **141**, 457 (1977).

[13]W. Bertozzi *et al.*, Nucl. Instrum. Methods **162**, 211 (1979).

[14]J. W. Lightbody *et al.*, Phys. Rev. C **14**, 952 (1976).

[15]G. L. Detch *et al.*, Phys. Rev. C **4**, 52 (1971).

[16]D. M. Skopik *et al.*, Phys. Rev. C **24**, 1791 (1981).

[17]J. C. Bergstrom, in Medium Energy Nuclear Physics with Electron Linear Accelerators, edited by W. Bertozzi and S. Kowalski, U.S. Atomic Energy Commission Publication TID-24667, 1967 (unpublished).

[18]L. M. Mo and Y. S. Tsai, Rev. Mod. Phys. **41**, 205 (1969).

[19]L. S. Cardman *et al.*, Phys. Lett. **91B**, 203 (1980).

[20]B. Dreher *et al.*, Nucl. Phys. **A235**, 219 (1974).

[21]G. Retzlaff and D. M. Skopik, Phys. Rev. C **29**, 1194 (1984).

[22]For example, G. R. Payne, J. L. Friar, and B. E. Gibson, Phys. Rev. C **22**, 832 (1980).

[23]L. I. Schiff, Phys. Rev. **133**, B802 (1964).

[24]S. A. Coon (private communication).

[25]J. L. Friar *et al.*, Phys. Rev. C **24**, 665 (1981).